Numerical Analysis of the FDA Centrifugal Blood Pump

V. Marinova, I. Kerroumi, A. Lintermann, J. H. Göbbert,
C. Moulinec, S. Rible, Y. Fournier, M. Behbahani

published in

NIC Symposium 2016
K. Binder, M. Müller, M. Kremer, A. Schnurpfeil (Editors)

Forschungszentrum Jülich GmbH,
John von Neumann Institute for Computing (NIC),
Schriften des Forschungszentrums Jülich, NIC Series, Vol. 48,
ISBN 978-3-95806-109-5, pp. 355.
http://hdl.handle.net/2128/9842

Numerical Analysis of the FDA Centrifugal Blood Pump

Valeria Marinova[1], Iman Kerroumi[1], Andreas Lintermann[2], Jens Henrik Göbbert[2], Charles Moulinec[3], Sebastian Rible[1], Yvan Fournier[4], and Mehdi Behbahani[1]

[1] University of Applied Sciences Aachen, Campus Jülich,
Heinrich-Mußmann-Straße 1, 52428 Jülich, Germany
E-mail: {valeria.vereshchagina, iman.kerroumi}@alumni.fh-aachen.de, behbahani@fh-aachen.de

[2] Jülich Aachen Research Alliance (JARA-HPC), RWTH Aachen University,
Schinkelstraße 2, 52062 Aachen, Germany
E-mail: {lintermann, goebbert}@jara.rwth-aachen.de

[3] Scientific Computing Dept. Science and Technology Facilities Council Daresbury Laboratory,
Sci-Tech Daresbury Warrington, WA4 4AD, United Kingdom
E-mail: charles.moulinec@stfc.ac.uk

[4] EDF - R&D Fluid Mechanics, Energy and Environment Department,
6 quai Watier - BP 49, 78401 CHATOU Cedex, France
E-mail: yvan.fournier@edf.fr

Ventricular Assist Devices (*VADs*) are commonly implanted to assist patients suffering from heart diseases. They provide long- and short-term support for the human heart and help patients to recover from heart attacks and from congestive heart failure. It is essential to design blood-sensitive *VADs* to minimise the risk of hemolysis and thrombosis. The blood pump, however, must operate at a wide range of flow rates and pressure heads which makes a low-risk design a challenging task. In this study the flow in a centrifugal blood pump, provided by the *U.S. Food and Drug Administration* (*FDA*), is investigated by means of numerical simulations on high performance computers. The simulations are carried out for different operation REYNOLDS numbers. A total of 15 pump revolutions is performed to obtain quasi-steady results. The pressure drop across the pump is considered to study convergence of the solution and to characterise the energy loss of the device. Investigations of the velocity field show that there exist high velocities and strong velocity gradients and shear layers in the outflow region potentially leading to hemolysis. Investigations of the wall-shear stress reveal the existence of thin boundary layers at the blade tips. Finally, the motor torque is investigated to identify the force acting on the blades. All the findings show that there is a strong need to develop more blood-sensitive designs to reduce the risk of hemolysis and thrombosis.

1 Introduction

In 2014, about 26 million people worldwide suffered from heart failure[1], which is the most common fatal disease in developed countries. Heart failure develops gradually as the heart muscle weakens. It is caused by a dysfunction of the heart's ventricle that limits the cardiac performance and can often only be treated by heart transplant. However, only 5,000 donor hearts become available each year, while 50,000 patients remain waiting[2].

Ventricular Assist Devices (*VADs*) are the only viable bridging solution allowing patients to survive until a donor is found. Such devices consist of inflow and outflow cannulas and a blood pump to support the ventricle pumping. The major advantage, e.g., over a *Total Artificial Heart* (*TAH*), is that the native heart remains in the body while the *VAD* sustains the natural blood flow by means of an external power supply. Two different major kinds

of blood pumps exist, i.e., axial and centrifugal pumps. Axial blood pumps consist of a rotor type impeller mounted in a small housing rotating at $8{,}000 - 15{,}000\ \mathrm{rpm}$ [3]. Thereby, the pump accelerates the blood in the streamwise direction based on the principle of the Archimedean screw. High rotational speed may lead to non-physiological flow conditions, i.e., high shear stress and the formation of recirculation zones. Such phenomena may induce hemolysis and thrombosis. High shear rates may damage the red blood cells causing excessive hemolysis which may lead to kidney and hence multiple organ dysfunction. The formation of recirculation zones increases the likelihood of blood clots, which may circulate in the cardiovascular system and obstruct important arteries or veins. In contrast to axial pumps, centrifugal pumps operate at a speed of $1{,}400 - 4{,}000\ \mathrm{rpm}$ and consist of a non-occlusive pump head with several rotor blades mounted in a pump housing[4]. The fluid enters through the head and is centrifugally accelerated by the perpendicularly mounted pump head. The accelerated flow decelerates in the diverging outflow cannula causing a pressure increase. As fluid is displaced at the discharge side of the pump, more fluid is sucked in to replace it at the suction side leading to flow[5].

Blood pumps must operate over a wide range of flow rates and pressure heads. Another requirement is minimisation of the damage to blood cells. The intricacy of the problem makes *Computational Fluid Dynamics* (*CFD*) a powerful tool for the analysis and design of blood pumps. A review of the design and numerical analysis of both centrifugal and axial blood pumps is given in Behbahani *et al.*[6].

The investigations in this study concentrate on a centrifugal blood pump provided by the *U.S. Food and Drug Administration* (*FDA*). The *FDA* aims at characterising the feasibility of *CFD* methods for the design of medical devices. That is, they review the disadvantages and problems of medical devices and call health professionals' attention to their findings. At the end of 2013 the *FDA* invited academical as well as industrial organisations of the *CFD* community to take part in a benchmark study that involves the analysis of the flow in a typical blood pump. The study is composed of six test cases with different pump speeds and REYNOLDS numbers in the range of $Re = 210 \cdot 10^3$ to $Re = 293 \cdot 10^3$. The high REYNOLDS number regime requires large meshes to highly resolve the flow and *High Performance Computing* (*HPC*) is mandatory to perform the simulations. They have been carried out on the JUQUEEN[7] system at the *Jülich Supercomputing Centre* (*JSC*). Within this work, the velocity field, secondary flow structures, the wall-shear stress, and the motor torque are investigated to develop an understanding of the blood sensitivity of the *FDA* blood pump. For validation of the numerical results the *FDA* has contracted 3 independent laboratories to produce experimental data of the flow through the pump by means of *Particle Imaging Velocimetry* (*PIV*).

This paper is organised as follows. The numerical method for the simulation of the flow in the centrifugal *FDA* blood pump and the code scalability are described in Sec. 2. Subsequently, the results of the simulations at several REYNOLDS numbers are presented in Sec. 3. Finally, conclusions are drawn in Sec. 4.

2 Numerical Methods

In this section the numerical methods, i.e., the flow solver, the geometry of the problem and the mesh generation as well as a scalability analysis of the simulation code are presented.

2.1 Flow Solver

To simulate the flow in the *FDA* centrifugal blood pump a *Finite Volume Method* (*FVM*) is used since it is well suited for *CFD* simulations of high REYNOLDS number flows in complex geometries. In addition, *FVM* is known to demonstrate good parallel performance[8].

Code_Saturne[a] implements these advantages and is well suited for three-dimensional calculations of steady or transient single-phase, incompressible or compressible, laminar or turbulent flows[9]. Advanced and accurate turbulence modelling for *Reynolds-Averaged Navier-Stokes* (*RANS*) and *Large-Eddy Simulations* (*LES*) represents a key feature of the code. Its flow solver is based on a *FVM*, with a fully co-located arrangement for all variables and a predictor-corrector scheme for the time discretisation of the Navier-Stokes equations. Parallelisation is handled using *MPI*, and some *OpenMP* pragmas are implemented in version 3.2.x and 3.3.x of the code. *Code_Saturne* is developed since 1997 at EDF R&D and has found massive application for a variety of fluid mechanical problems on several high-end machines[10].

Within the framework of this study several *RANS* turbulence models were tested including first order models such as k-ϵ and k-ω and, a *Reynolds Stress Model* (*RSM*), namely the *Rij-SSG (Speziale, Sarkar, Gatzki)*[11,12]. It was shown that the *RSM* represents an appropriate choice with respect to modeling high-REYNOLDS number flow cases as isotropic first order models (k-ϵ, k-ω) without rotation correction do not correctly model turbulence effects with rotation, which induces anisotropy.

2.2 Geometry and Mesh Generation

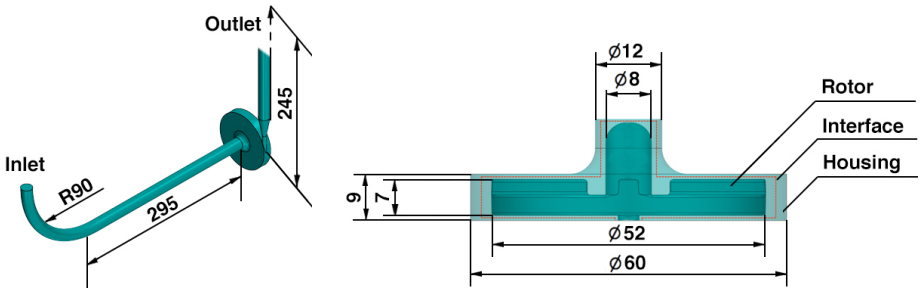

Figure 1. a) Picture of the *FDA* centrifugal blood pump, showing the long curved inlet, the pump and a part of the long outlet; b) cross section of the pump including dimensions and interface (red line) between the rotor and the housing which separates the rotating and static flow regions. All dimensions are given in mm.

The *FDA* centrifugal blood pump consists of two main components: the housing and the rotor positioned inside it. The blood flows through a curved inlet tube into the housing interior, where it meets a hub and then is rotated within the interior of the housing by means of the rotor. Finally, blood exits the pump through a diffuser and continues into the outlet (see Fig. 1).

[a] `http://www.code-saturne.org/`

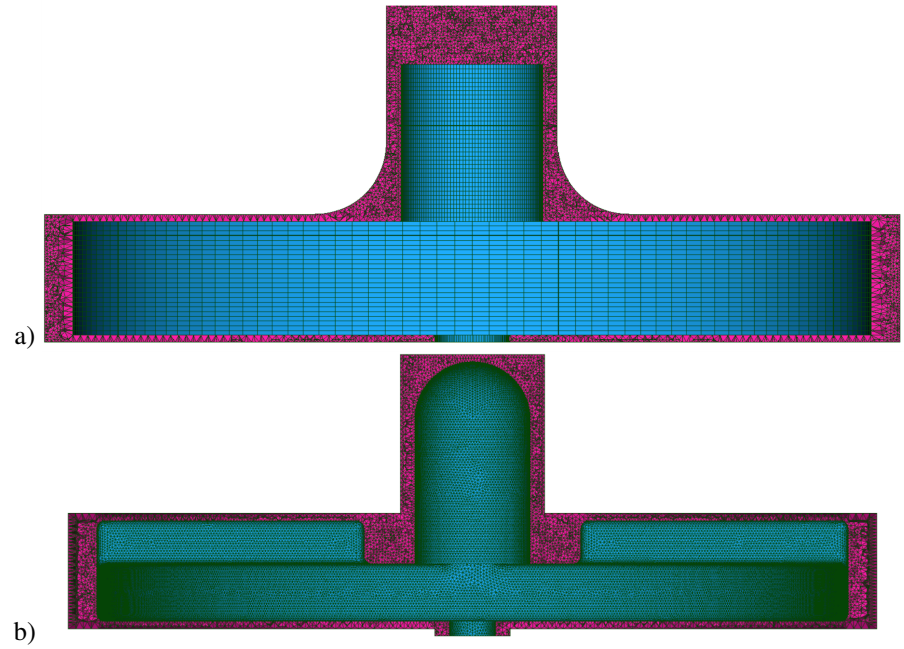

Figure 2. Cross-sectional view (in purple) of a) static domain and b) dynamic domain meshes. At the interface region pyramids can be seen.

For the grid generation SALOME version 6.6.0 [b] was used. To be able to simulate the motion of the rotor, an interface is introduced and the mesh is split into two sub-meshes, one for the rotor (which is moving) and one for the stator (which is static). The first sub-mesh consists of the mesh of the rotor in a cylinder, and the second sub-mesh of the mesh of the rest of the geometry minus the aforementioned cylinder (see the interface in Fig. 1 b). An efficient and fully parallel mesh joining strategy is used at each time step between both sub-meshes to create a full mesh used to solve the *RANS* equations. Hybrid meshes were generated consisting of pyramids and tetrahedra, which had a defined number of regularly arranged quadrangular surface elements at the interface. The corresponding sub-meshes are shown in Fig. 2. The pump region, i.e., the first sub-mesh, was made of 14 million cells at first and was later refined to 21 million cells for better resolution of critical areas. The final full mesh including also the long inlet and outlet contained a total of 76 million cells. The cell volume ranged between $5.05 \cdot 10^{-15}\text{m}^3$ and $9.14 \cdot 10^{-12}\text{m}^3$. The mesh was designed fine enough to serve for the production runs of the *FDA* simulations, and scalable wall-functions were used to better capture boundary layers. The same 76 million cell mesh was used for all 6 simulations (see Tab. 1), which were conducted on the IBM Blue Gene/Q JUQUEEN at Jülich Supercomputing Centre[13].

After computing the flows using the *Code_Saturne* version 3.2.x, the flow structures are visualised using ParaView[14] version 3.14.1.

[b] `http://www.salome-platform.org/`

2.3 *Code_Saturne* Scalability Study

Code_Saturne has demonstrated extreme scalability up to 1,572,864 *MPI* tasks, using 32 ranks per node on the IBM Blue Gene/Q Mira, Argonne National Laboratory. Fig. 3 shows the speed-up of *Code_Saturne* for three mesh sizes, consisting of 111 million, 889 million, and 13 billion cells, respectively. The first two meshes (blue and green solid lines respectively) have been run for the classical lid-driven cavity test case, using tetrahedral cells. The third test (red solid line) is based on a mesh made of hexahedral cells and was designed for *LES* in tube bundles.

A scalability study was also performed for this case and included test runs for all 6 cases which *FDA* asked for. Effects of partitioning algorithms on the scalability were also investigated, using either serial METIS[15] or PT-Scotch[16]. For a number of 1,024 - 65,536 processors METIS turned out to be the most efficient partitioner, requiring 11.7 seconds to compute one iteration.

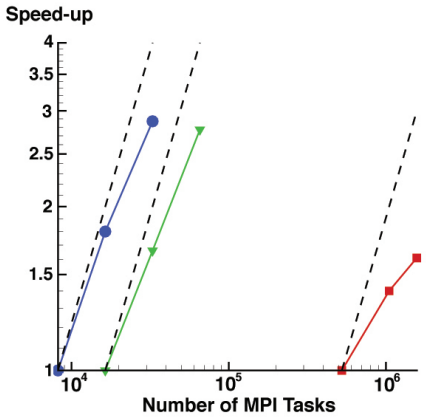

Figure 3. Speed-up of *Code_Saturne* on Blue Gene/Qs, as a function of the number of *MPI* tasks. The blue (111M cells) and green (889M cells) plots with respectively circle and triangle symbols are obtained on Blue Joule (Hartree Centre, STFC, UK) and the red (13B cells) plot (square symbols) on Mira (DOE, Argonne, US).

3 Results of the Centrifugal Pump Analysis

Similar to the REYNOLDS number definition for stirred vessel flow, the *FDA* defined the REYNOLDS number as $\mathrm{Re} = \rho v 2\pi d^2/\eta$, where $\rho = 1035.0\ \mathrm{kg/m^3}$ is the blood density, v is the respective pump's rotational speed, $d = 0.052\ \mathrm{m}$ is the rotor diameter and $\eta = 0.0035\ \mathrm{Pa}$ is the blood viscosity. Blood is known to display non-Newtonian properties[17]. However, in experimental studies[18] it has been shown that at shear rates $\dot{\gamma} > 100\ \frac{1}{\mathrm{s}}$, the viscosity of human blood with physiological hematocrit reaches a constant value, thus justifying the choice of a Newtonian model at moderate and high shear rates. The according flow conditions for all 6 cases are listed in Tab. 1. The data files which had to be

Case	volume flow rate [L/min]	pump speed [*rpm*]	REYNOLDS number
1	2.5	2500	293,073
2	2.5	3500	209,338
3	4.5	3500	293,073
4	6.0	2500	209,338
5	6.0	3500	293,073
6	7.0	3500	293,073

Table 1. Standard setup parameters of the blood pump benchmark as defined by the *FDA*.

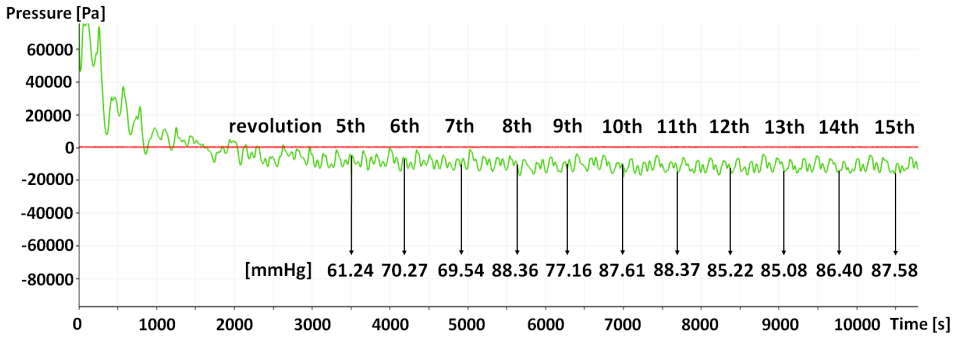

Figure 4. Pressure evolution as a function of time for 15 revolutions for the example of simulation case 6. Pressure values averaged over a full revolution are given in units of mmHg. The red curve represents *zero*-pressure at the outlet and the green curve shows the pressure at the inlet.

submitted to the *FDA* included velocities and pressures in the blade passage plane and in the outlet plane for all 6 simulation cases for prescribed rotor positions.

Depending on the flow case a fixed time step of $2.45 \cdot 10^{-5}$s or $3.43 \cdot 10^{-5}$s was applied for typically 10,500 iterations in order to compute 15 revolutions of the rotor to approach a quasi-stationary state which is shown in Fig. 4 for simulation case 6. The computational effort (used CPU time) for computing one revolution of the blood pump while typically using 32,768 MPI tasks for the 76 million cell mesh resulted in 11,279s or 3h 13min. It can be observed that the solution converges towards a quasi-steady state and that the averaged pressures over each revolution approach near-constant values, where a value of $80 - 90\mathrm{mmHg}$ corresponds to physiological pressure ranges.

Velocity and wall shear stress distributions for flow case number 5 are shown in Fig. 5. The highest overall velocities are found in the narrow portion of the diffuser at the pump outlet.

Fig. 6 shows the velocity field inside the blood pump housing. Inside the pump the highest velocities occur behind the rotor blades. From the representation by means of velocity vectors it can be observed that once the fluid has left the low-velocity inflow region, fluid particles follow a circumferential path. Strong radial components are only visible closely behind the rotor blades. Centrifugal forces pushing the particles to the outside are adding an additional radial velocity component in the wake of the blades. The pressure

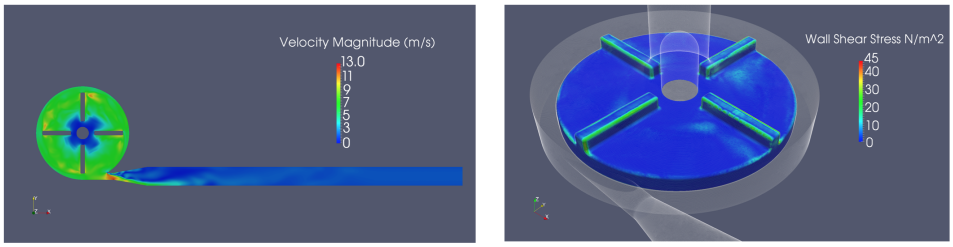

Figure 5. Velocity distribution in the x,y-plane (left) and wall shear stress at the rotor surface (right) for simulation case 5.

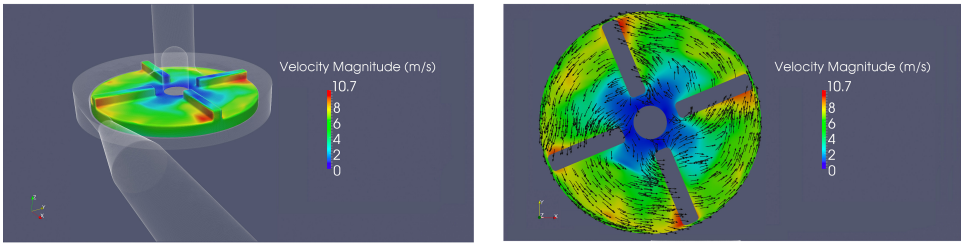

Figure 6. Velocity field inside the *FDA* blood pump housing (left) and velocity vector distribution at close proximity to rotor surface (right) for simulation case 6. Rotor rotates in anti-clockwise direction.

loss caused by the velocity increase further accelerates particles in that region. The pressure distribution (data not shown here) in the pump clearly shows low pressures behind blade tips and high values in front of the tips and thereby confirms this interpretation. Another explanation for the elevated velocity values could be that there exist tip vortices in the wake of the pump blades that rotate at high velocities, which add velocity behind the blade. However, it is possible that *RANS* cannot capture these structures and *LES* computation and analysis is necessary in the future studies.

Tab. 2 shows a summary of characteristic pressure, wall shear stress and torque values. The given pressure head values represent the time-averaged pressure difference between

Case	pressure head $[10^3 \mathrm{N/m^2}]$	wall shear stress $[\mathrm{N/m^2}]$	shaft torque $[10^{-3}\ \mathrm{Nm}]$
1	77.6	61.2	8.4
2	49.3	27.4	13.3
3	38.6	135.5	18.8
4	-5.1	72.9	15.9
5	24.4	129.0	24.5
6	14.9	119.8	26.7

Table 2. Time-averaged pressure head (between inlet and outlet) over last rotation, time-averaged wall shear stress magnitude over the housing rim and shaft torque for all 6 *FDA* simulation cases.

the outlet and inlet. To that purpose pressure values were averaged over the inlet and outlet areas respectively for a given rotor position. The time-averaged wall shear stress magnitude was computed over the housing rim and was averaged over the last full rotation. Finally, the torque values were computed from the velocity derivatives acting parallel to the rotor surface and pressures perpendicular to the blades. According to the computed values for the pressure head, simulation case 4 is not a feasible operating condition as a very low and negative pressure would not support the required pumping function. All other cases represent operating conditions, where the computed pressure heads lie in the range of typical values reported in literature[19]. Values found for commercial blood pumps lie typically in a range of $80\ \mathrm{mmHg} - 200\ \mathrm{mmHg}$ ($10{,}666 - 26{,}666 Pa$) but can go up to values of $700\mathrm{mmHg}$ ($93{,}331 Pa$) depending on the operating conditions. The computed wall shear stress values are especially high for the simulation cases 3, 5 and 6. Values between $119.8 - 135.5 Nm$ may cause hemolysis, especially because in centrifugal blood pump the blood does not necessarily leave the pump after the first rotation. The blood may rotate several times inside the housing, which strongly increases the shearing time for blood cells and can cause strong deformation or rupture of these cells.

Post-processing and visualisation of the simulation data were performed on local computers for distinct time steps and on JUVIS at the *JSC* if many time steps had to be loaded simultaneously. Besides the various pictures requested by the *FDA*, it was possible to produce dynamic visualisation of the data including a movie of the blood flow situation inside the *FDA* pump for the 76 million cell mesh. A snapshot from that movie is shown in Fig. 7. About 1000 frames were generated through ParaView which amounts for over two and a half revolutions. Pathline generation (not shown here) could also be performed.

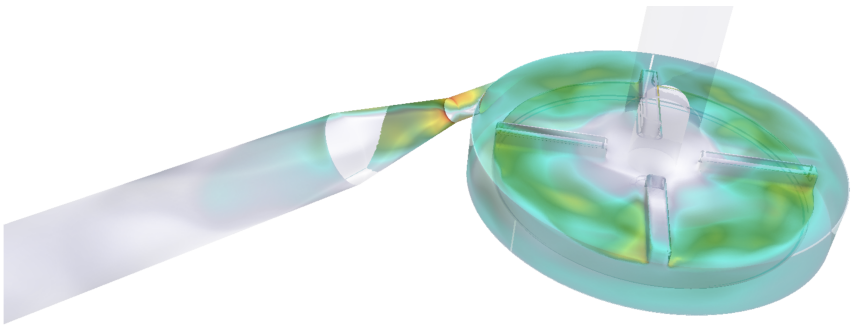

Figure 7. Screenshot from a movie which was made for the 76 million mesh visualising the flow inside the *FDA* blood pump. Colours represent the velocity magnitude. Rotor rotates in anti-clockwise direction.

4 Conclusion and Outlook

In this study the blood flow could be characterised for different operating conditions of the *FDA* centrifugal blood pump. High shear stress regions could be identified both inside the housing and in the diffusor region. The high shear values detected for some of the flow cases may lead to hemolysis. The presented *CFD* study results can therefore serve

to improve existing centrifugal blood pumps to obtain a hemocompatible design. The required shaft torque, an important characteristic value for the operation of a centrifugal blood pump, could equally be determined. All quantitative data and visualisations required for the benchmark could be sent to the *FDA*. The performed flow field characterisation can serve in the future to quantitatively estimate hemolysis using a mathematical model of red blood cell deformation and damage. In the context of this study, *Code_Saturne* could be shown to be an efficient, scalable code which is suitable for the analysis of highly turbulent rotating flows.

One important next step will be to compare the numerical results with real measurements. Until now the *FDA* has not yet published any experimental results from the three laboratories that were asked to perform comparative *PIV* studies but the publication of such results is expected soon. From comparison to literature and from analytical considerations it can already be concluded that the computed results are of the right order.

Another next step will be to perform *Large-Eddy Simulations (*LES) for the *FDA* blood pump. *LES* computations will essentially help to understand the unsteady and highly dynamic flow in blood pumps and will support design studies for future *VADs*. The findings will help to reduce the high shear stress in such devices and will hence minimise the risk of hemolysis and thrombosis for the patient. These studies represent a step towards the establishment of reliable methods to accurately predict blood flow and blood damage in fast rotating biomedical devices. The *LES* computations will increase the computational complexity and will at the same time require finer meshes of approximately 200 million elements to capture turbulent effects, thus making the continued use of high performance computing necessary.

Acknowledgements

We would like to thank G. Groten for many fruitful discussions on the intricacies of Fortran 90 and for the coding of a significant part of the interface library.

The authors gratefully acknowledge the *Gauss Centre for Supercomputing* (*GCS*) for providing computing time through the *John von Neumann Institute for Computing* (*NIC)* on the *GCS* share of the supercomputer JUQUEEN[7] at the *JSC*.

Furthermore, the authors thank the Simulation Laboratory "Highly Scalable Fluids & Solids Engineering" and the Cross-Sectional Group "Immersive Visualisation" of the *Jülich Aachen Research Alliance, High Performance Computing* (*JARA-HPC*) and *JSC*.

The authors would also like to thank the Hartree Centre for using their Blue Gene/Q to generate data for the film and the INCITE PEAC programme of the US DOE for letting them perform extreme scalability studies using MIRA.

References

1. P. Ponikowski, S. D. Anker, K. F. AlHabib, M. R. Cowie, T. L. Force, S. Hu, T. Jaarsma, H. Krum, V. Rastogi, L. E. Rohde, U.C Samal, H. Shimokawa, B. Budi Siswanto, K. Sliwa, and G. Filippatos, *Heart Failure: Preventing Disease and Death Worldwide*, ESC Heart Failure **1**, 4-25, 2014.

2. D. O. Taylor, L. B. Edwards, M. M. Boucek, E. P. Trulock, P. Aurora, J. Christie, F. Dobbels, A. O. Rahmel, B. M. Keck, and M. I. Hertz, *Registry of the International Society for Heart and Lung Transplantation: Twenty-fourth Official Adult Heart Transplant Report-2007*, Journal of Heart and Lung Transplantation **8**, 769-781, 2007.
3. D. L. Mann, D. P. Zipes, P. Libby, R. O. Bonow, *Braunwald's Heart Disease: A Textbook of Cardiovascular Medicine* Elsevier **10**, 596, 2015.
4. A. D. Kirk, S. J. Knechtle, C. P. Larsen, J. C. Madsen, T. C. Pearson, S. A. Webber, *Textbook of Organ Transplantation Set* Wiley **10**, 559, 2015.
5. C. Allerstorfer, *Centrifugal Pumps* MU Leoben, 2013.
6. M. Behbahani, M. Behr, M. Hormes, U. Steinseifer, D. Arora, O. Coronado, M. Pasquali, *A Review of Computational Fluid Dynamics Analysis of Blood Pumps* European Journal of Applied Mathematics **20**, 363-397, 2009.
7. Jülich Supercomputing Centre, *JUQUEEN: IBM Blue Gene/Q Supercomputer System at the Jülich Supercomputing Centre*, Journal of large-scale research facilities **1**, A1, 2015.
8. Y. Fournier, J. Bonelle, C. Moulinec, Z. Shang, A. G. Sunderland, and J. C. Uribe, *Optimizing Code_Saturne computations on petascale systems*, Computers and Fluids **45**, 103-108, 2011.
9. F. Archambeau, N. Méchitoua, and M. Sakiz, *Code_Saturne: A finite volume code for the computation of turbulent incompressible flows-Industrial applications*, International Journal on Finite Volumes **1**, 1, 2004.
10. C. Moulinec, D. R. Emerson, Y. Fournier and P. Vezolle, *Challenges to be Overcome for Engineering Software to Run Efficiently on Petascale Machines*, in B.H.V. Topping and P. Ivanyi - Saxe-Coburg Publications, 23-40, 2013.
11. C. Speziale, T. Gatski, and N. Mhuiris, *A critical comparison of turbulence models for homogenous shear flows in a rotating frame*, Physics of Fluids **9**, 1678-1684, 1990.
12. C. Speziale, S. Sarkar, and G. Gatski, *Modeling the pressure strain correlation of turbulence - an invariant dynamical systems approach*, Journal of Fluid Mechanics **227**, 245-272, 1991.
13. Jülich Supercomputing Centre, *JUQUEEN: IBM Blue Gene/Q Supercomputer System at the Jülich Supercomputing Centre*, Journal of large-scale research facilities **1**, 1-18, 2015.
14. U. Ayachit, *The ParaView Guide: A Parallel Visualization Application, Kitware, ISBN 978-1930934306*, 2015.
15. G. Karypis and V. Kumar, *A Fast and High Quality Multilevel Scheme for Partitioning Irregular Graphs*, SIAM Journal on Scientific Computing **20**, 359, 1998.
16. C. Chevalier and F. Pellegrini, *PT-Scotch: A tool for efficient parallel graph ordering*, Parallel Computing **34**, 318-331, 2008.
17. P. Easthope and D. Brooks, *A comparison of rheological and constitutive functions for whole human blood*, Biorheology **17**, 235-247, 1980.
18. S. Chien *Shear dependence of effective cell volume as determinant of blood viscosity*, Science **168**, 977-979, 1970.
19. K. Franco and E. Verrier, *Advanced Therapy in Cardiac Surgery*, in PMPH USA 2nd edition, 2013.